Communications on Applied Nonlinear Analysis
ISSN: 1074-133X
Vol 31 No. 7s (2024)

Computational Framework on MHD Hybrid Nanofluid Flow Over A Stretching Surface with Thermal Radiation

G. Kavitha[1], S. H. Manjula[2*]

[1,2] Department of Mathematics (S and H), Vignan's Foundation for Science, Technology & Research (VFSTR), Vadlamudi, Guntur, Andhra Pradesh −522213, India.

*Corresponding author Email: Manjubknd.bk@gmail.com

Article History:

Received: *01-06-2024*

Revised: *03-07-2024*

Accepted: *29-07-2024*

Abstract:

Nanofluids improve heat transmission in a variety of sectors, including automotive production, medical care, solar power, and technology. In the presence of a magnetic field, a comparative examination of hybrid nanofluids is investigated. Porous media and heat radiation are the new issues that are being investigated in the present study. Thermal energy serves as the foundation of motivation for hybrid nanofluid delivery, which is discussed in this article. By applying the compatible similarity functions, the higher-order PDEs are renewed into a couple of ordinary differential equations. The MATLAB platform via bvp5c code is used for numerical technique. A trustworthy comparison with previously published literature is carried out in order to ensure the correctness and validity of the findings. The graphical results for various profiles, such as velocity and energy, are shown for various important active parameters. It is perceived that by increasing the magnetic parameters M and Pr, the velocity and temperature of the fluid decrease, respectively. Specifically, the results of this work contribute to the advancement of understanding in the field of MHD as well as heat transfer mechanisms. Furthermore, the learnings that were obtained have the ability to improve the effectiveness and performance of thermodynamic systems across different kinds of applications, including those in the industrial and medical fields.

Keywords: MHD, Thermal radiation, Porous medium, Hybrid nanofluid, bvp5c.

1. Introduction

Engineering and science are increasingly focused on controlling the small-scale and nanometer characteristics of the fluids that are used. During the 1990s, nanofluids developed. The most exacting uses of nanofluids are an important issue in the scientific and technical communities. Nanofluid simulations were studied from multiple perspectives by scientists due to the widespread use of nanotechnology in modern science. To create nanofluids, tiny particles with sizes ranging from 1 to 100 nanometers have been suspended in a regular fluid. In terms of form, the tiny particles are spherical in shape. The dimension of tiny particles is intentionally kept so small due to the fact that, in comparison to big nanoparticles of identical weight, tiny particles have a larger surface region. This is the explanation for why particles are so tiny. Since we are aware that the amount of ion emission through the outermost region is proportional to the dimension of the surface, we may deduce that the bigger the cover area, the higher the electron emission [1] [2] [3]. The fact that tiny particles, despite their little size, discharge larger amounts of ions every unit mass than bigger particles gives them a greater antibiotic impact [4] [5] [6].

Hybrid nanofluids, which are a combination of two different kinds of nanoparticles that are distributed over a base fluid, are an innovative contemporary form of nanofluid that is being launched in the industry later on. This nanofluid is acknowledged as having the ability to effectively increase heat transmission. The research conducted demonstrates that this novel type of fluid has a significant improvement in its ability to conduct heat transfer. It would seem that there are not a lot of studies that are conducted on hybrid nanofluids. As a result, the primary objective of this inquiry is to investigate the dynamics of a hybrid nanofluid in a deformable sheet, namely the stretching and shrinking of the nanofluid. Because their uses are widely known in manufacturing sectors, particularly in plastic preparation, optical fiber manufacturing, chilling and drying of paper, and many other sectors, it is essential to highlight that deformable sheets are not a new critical issue among researchers in the fluid area. This is something that should be taken into consideration [7] [8] [9].

Over the course of the last several years, a number of scientists and analysts have been motivated to conduct magneto-hydrodynamic investigations. Within this context, magnetohydrodynamics, often known as MHD, is the technical control that investigates the magnetic behavior of fluids that conduct electricity, such as plasmas, seawater, fluid metals, and ions. This kind of thinking is helpful in many fields, including magnetic resonance imaging, bloodstream expressing, RFA, tumor malignancy therapy, cooling processes in nuclear power plants, metalworking thermal safeguarding of acquiring and sending devices, magnetic electro-catalysis, and many more. The mechanism of heat transmission that occurs when instantaneous energy is released from a material that has a temperature that is greater than absolute zero is referred to as the transmission of heat radiation. Heat radiation may be divided into two categories: linear and nonlinear radiation. Many different types of manufacturing and space-related products and processes involving high temperatures rely on heating phenomena, including liquid-bed temperature reactors, spacecraft, rockets, sunlight, nuclear power plants, propellers for aircraft components, engines for combustion, solar panels, and shining structures. [10][11][12].

According to the current literature, the simultaneous effects of MHD, porous medium, and heat generation across a stretching surface have been illustrated, and all are considered in the model. As per the author's knowledge, this kind of model has not been examined before. Equations in the form of PDEs are generated as a result of this process. With the help of self-similarity transformation, the PDEs are converted into ODEs. We used water as a foundation fluid in our investigation, and the hybrid nanofluids that we use are Al2O3-Cu. After applying transformations, for graphical purposes, we have used the numerical method, which is the bvp5c procedure in the MATLAB solver. Various graphs representing physical importance are provided in the results and discussion parts. Practical applications in the water purification industry have made use of the present study.

2. Mathematical model

A steady 2D flow of hybrid nanofluid with thermal heating induces by stretching surface is investigated. Following assumptions are deliberated:

- Induced magnetic field B is perpendicular to the sheet.
- (u,v) are velocity components.

- MHD and Porous medium are considered in flow problem.
- The behavior of the flow is linear.
- For motivation the MHD and thermal radiation is studied.
- Two distinct kinds of nanoparticles, namely Al_2O_3-Cu, are suspended in the base fluid Water which is considered in the present investigation.

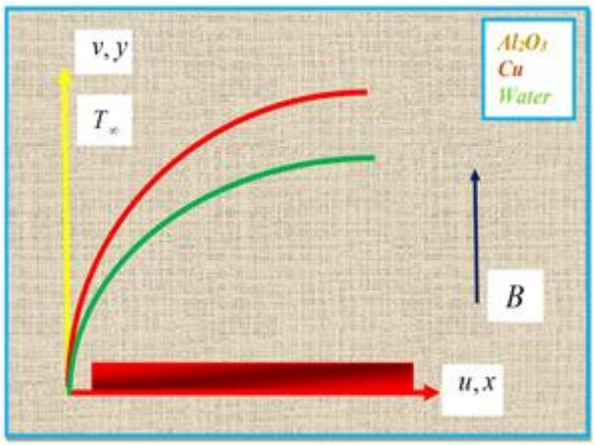

Fig – 1. Flow geometry of the problem.

The mathematical flow equations are [13], [14], [15]

$$\frac{\partial u}{\partial x}+\frac{\partial u}{\partial y}=0, \tag{1}$$

$$u\frac{\partial u}{\partial x}+v\frac{\partial u}{\partial y}=\frac{\mu_{hnf}}{\rho_{hnf}}\left(\frac{\partial^2 u}{\partial y^2}\right)-\frac{\mu_{hnf}}{\rho_{hnf}}\frac{u}{K^*}-\frac{\sigma_{hnf}}{\rho_{hnf}}\left(B^2u\right), \tag{2}$$

$$u\frac{\partial T}{\partial x}+v\frac{\partial T}{\partial y}=\frac{k_{hnf}}{\left(\rho c_p\right)_{hnf}}\left(\frac{\partial^2 T}{\partial y^2}\right)-\frac{1}{\left(\rho c_p\right)_{hnf}}\left(\frac{\partial q_r}{\partial y}\right)+\frac{\sigma_{hnf}B^2}{\left(\rho c_p\right)_{hnf}}u^2. \tag{3}$$

By Rosseland approach, we have

$$q_r=-\frac{4\sigma^*}{3k^*}\frac{\partial T^4}{\partial y}. \tag{4}$$

By applying the Taylor's series expansion of T^4 about T_∞ and neglecting terms having higher order, we obtain

$$T^4=4T_\infty{}^3T-3T_\infty{}^4. \tag{5}$$

By substituting Eq. (5) in Eq. (3), converted form is

$$u\frac{\partial T}{\partial x}+v\frac{\partial T}{\partial y}=\frac{k_{hnf}}{\left(\rho c_p\right)_{hnf}}\left(\frac{\partial^2 T}{\partial y^2}\right)-\frac{1}{\left(\rho c_p\right)_{hnf}}\frac{16T_\infty^3}{3k^*}\frac{\partial^2 T}{\partial y^2}+\frac{\sigma_{hnf}B^2}{\left(\rho c_p\right)_{hnf}}u^2. \tag{6}$$

The corresponding boundary conditions are:

$$\begin{aligned} &u = U = ax, v = 0, T = T_f, \quad at\ y = 0 \\ &u \to 0, T \to T_\infty \qquad\qquad as\ y \to \infty. \end{aligned} \tag{7}$$

The foll self-similarity transformations are:

$$u = axf'(\eta), v = -\sqrt{a\upsilon_f}\, f(\eta), \theta(\eta) = \frac{T - T_\infty}{T_f - T_\infty}, \eta = y\sqrt{\frac{a}{\upsilon_f}}. \tag{8}$$

Thermophysical properties of *hnf* are

$$G_1 = \frac{\mu_{hnf}}{\mu_f}, G_2 = \frac{\rho_{hnf}}{\rho_f}, G_3 = \frac{(\rho c_p)_{hnf}}{(\rho c_p)_f}, G_4 = \frac{k_{hnf}}{k_f}, G_5 = \frac{\sigma_{hnf}}{\sigma_f}.$$

$$\left.\begin{aligned} G_1 &= \frac{1}{(1-\phi_1)^{2.5}(1-\phi_2)^{2.5}}, \\ G_2 &= \left\{(1-\phi_2)\left[(1-\phi_1) + \phi_1\left(\frac{\rho_{s_1}}{\rho_f}\right)\right] + \phi_2\frac{\rho_{s_2}}{\rho_f}\right\}, \\ G_3 &= (1-\phi_2)\left[(1-\phi_1) + \phi_1\left(\frac{(\rho c_p)_{s_1}}{(\rho c_p)_f}\right)\right] + \phi_2\frac{(\rho c_p)_{s_2}}{(\rho c_p)_f}, \\ G_4 &= \frac{k_{s_1} + 2k_{bf} - 2\phi_2(k_{bf} - k_{s_2})}{k_{s_2} + 2k_{bf} + \phi_2(k_{bf} - k_{s_2})} \times \frac{k_{s_1} + 2k_f - 2\phi_1(k_f - k_{s_1})}{k_{s_1} + 2k_f + \phi_1(k_f - k_{s_1})}, \\ G_5 &= \frac{\sigma_{s_2} + 2\sigma_{nf} - 2\phi_2(\sigma_{nf} - \sigma_{s_2})}{\sigma_{s_2} + 2\sigma_{nf} + \phi_2(\sigma_{nf} - \sigma_{s_2})} \times \frac{\sigma_{s_1} + 2\sigma_f - 2\phi_1(\sigma_f - \sigma_{s_1})}{\sigma_{s_1} + 2\sigma_f + \phi_1(\sigma_f - \sigma_{s_1})}. \end{aligned}\right\} \tag{9}$$

Thus, when (8) is substituted, Equations (2, 6, and 7) have the following nondimensional form

$$\frac{G_1}{G_2} f''' + G_2\left(ff'' - (f')^2\right) - \frac{G_1}{G_2}Kf' - \frac{G_5}{G_2}Mf' = 0, \tag{10}$$

$$\theta''\left(G_4 + \frac{4}{3}Rd\right) + G_3 Prf\theta' + \frac{G_5}{G_3}MEc(f')^2 = 0. \tag{11}$$

The dimensionless boundary conditions are:

$$\begin{aligned} &f(0) = 0,\ f'(0) = 1, \theta'(0) = 1 \\ &f'(\infty) = 0, \theta'(\infty) = 0. \end{aligned} \tag{12}$$

$M = \frac{\sigma_f B^2}{\rho_f a}$ Magnetic field parameter
$Rd = \frac{4\sigma^* T_\infty^3}{k^* k_f}$ Radiation parameter

$K = \frac{\upsilon_f}{aK^*}$ Porosity parameter
$Ec = \frac{U^2}{c_p\left(T_f - T_\infty\right)}$ Eckert number
$Pr = \frac{\mu_f \left(c_p\right)_f}{k_f}$ Prandtl number

The dimensional form of C_f , and Nu are followed by

$$C_f = \frac{\tau_w}{\rho_f U^2} \tag{13}$$

Where τ_w is $\tau_w = \mu_{hnf} \left.\frac{\partial u}{\partial y}\right|_{y=0}$

$$Nu = \frac{x q_w}{k_f \left(T_w - T_\infty\right)} \tag{14}$$

Where q_w is $q_w = -k_{hnf} \left.\frac{\partial T}{\partial y}\right|_{y=0}$

The dimensionless form of Eqs. (13–14) are converted as

$$Re_x^{1/2} C_f = CF = G_1 f''(0), \tag{15}$$

$$Re_x^{-1/2} Nu_x = NU = -G_4 \theta'(0). \tag{16}$$

Where Re_r is the local Reynolds number.

3. Numerical scheme

To solve the highly non-linear ODE system of Eqs. (10)–(11), along with the boundary conditions (12), we have used the Bvp5c technique in the MATLAB solver. Firstly, Eqs. (10)–(12) is converted as a set of associated 1st-order equations so that Bvp5c may be employed in the MATLAB (R2020b) solver. In this particular investigation, the numerical findings are shown for a variety of distinct values of the variables that have been taken into consideration.

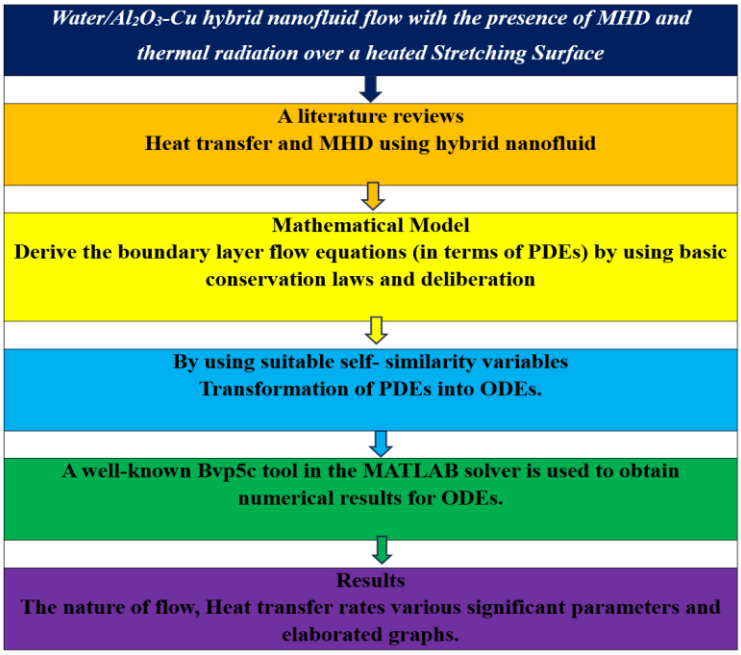

Fig – 2. Flow chart of the present investigation problem.

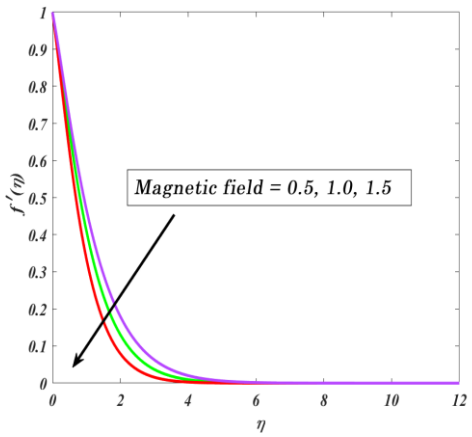

Fig – 3. Impression of M on $f'(\eta)$.

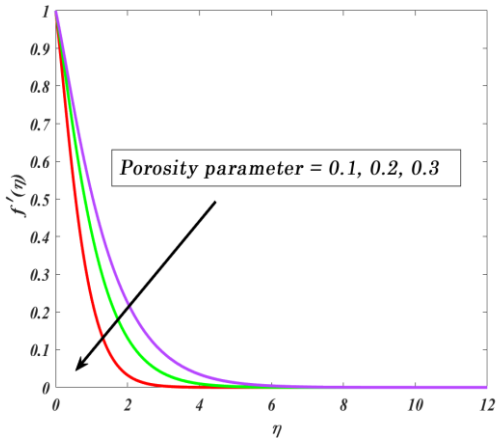

Fig – 4. Impression of K on $f'(\eta)$.

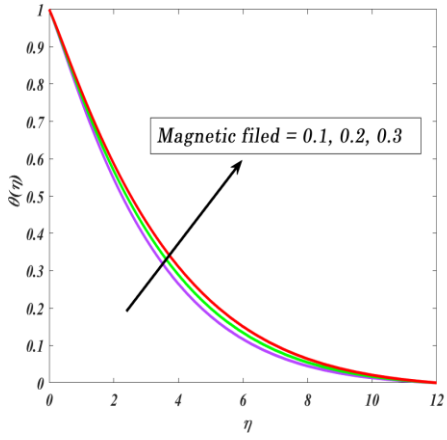

Fig – 5. Impression of M on $\theta(\eta)$.

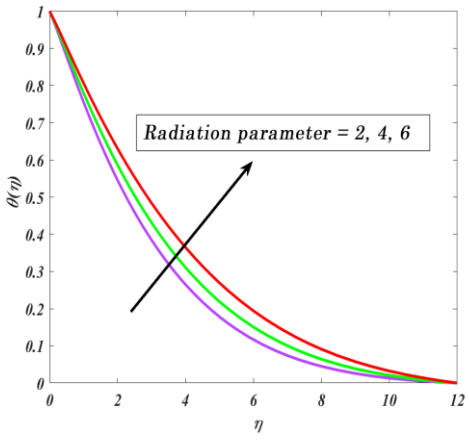

Fig – 6. Impression of Rd on $\theta(\eta)$.

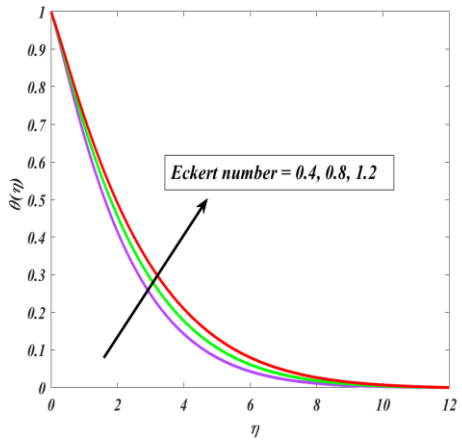

Fig – 7. Impression of Ec on $\theta(\eta)$.

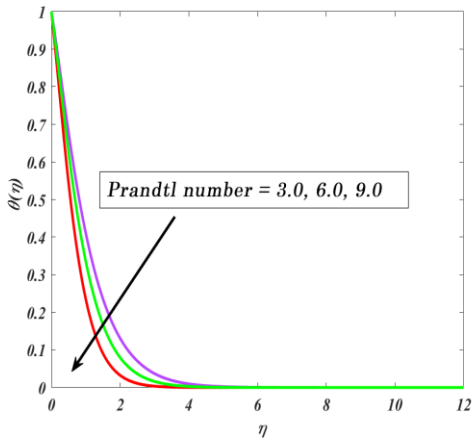

Fig – 8. Impression of Pr on $\theta(\eta)$.

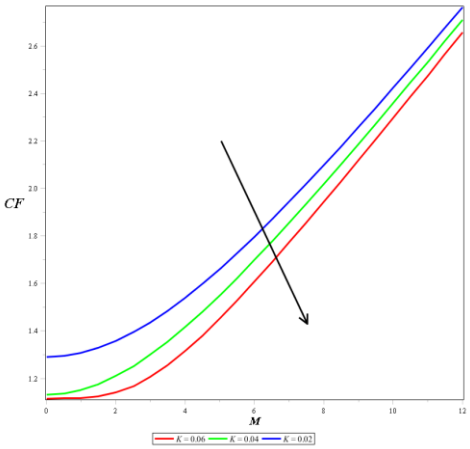

Fig – 9. Impression of K *and* M on CF.

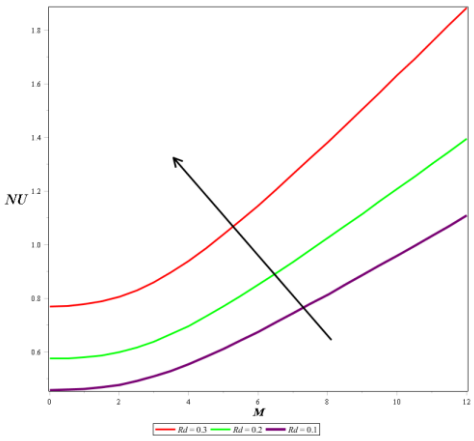

Fig – 10. Impression of Rd *and* M on NU.

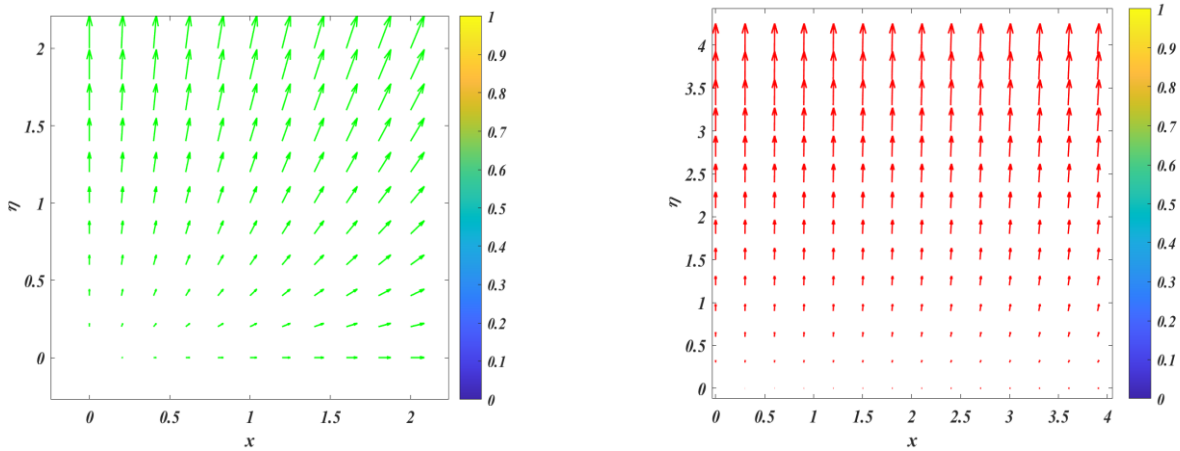

Fig – 11. Streamlines for different values of **(a)** M = 0.5 (Green), **(b)** M=1.0 (Red).

Table 1. Thermophysical properties of Water, Cu-Al_2O_3 hybrid nanofluid [16].

Parameter	*ρ (kg / m^3)*	*C_p (J / kgK)*	*k (W / mK)*	*σ (Ωm)$^{-1}$*	*Pr*
Water (H_2O)	997.1	4180	0.613	0.05	6.20
Copper (Cu)	8933	385	401	59.6×10^6	
Aluminium oxide (Al_2O_3)	3970	765	40	35×10^6	

4. Results and discussion

The non-dimensional controlling flow model (10)–(11), which is subject to the boundary conditions (12), may be solved numerically with the assistance of the Bvp5c scheme in MATLAB solver. We took the values of non-dimensional parameters and evaluated them. Table 2 provides accurate solutions, which demonstrate the variations in the Prandtl number. The results of both examinations were found to be reasonably accurate, according to the results.

The visual representation of the velocity is shown to be affected by M in Figure 3. There is a declining trend on the velocity graph, which indicates that M is increasing as it increases. In physical terms, the velocity of the fluid slows down as the force known as Lorentz is created by an increase in M. The Lorentz force makes it hard for liquids to accelerate, so the flow speed slows down because of additional resistance. This makes the field of motion smaller. Figure 4 shows that increasing the K values enhances the velocity profile. In practice, this is because a material that is porous gets harder to move through whenever the K values are raised, which retards the movement of fluids. A diminution in the size of the outermost layer of boundary walls is an instant and immediate impact of behavior.

Figure 5 shows the impact of M on the energy outline. An increase in the M parameter was found to result in an improvement in the energy contour. This improvement is a result of the fact that the incorporation of a M into a material that is electrically conductive results in the production of a force called Lorentz, which is resistance. There is the potential for such a type of force to cause the internal temperature of the liquid to increase. Consequently, this is the explanation why the temperature profile increased. Figure 6 illustrates the impact of the radiation parameter on the energy profile. This influence can be seen in the figure. The temperature picture will become more favorable as the amounts of the energy parameters continue to increase. From a physical standpoint, there is a connection between the greater amount of energy and the depth of the boundary layer of heat. This connection corresponds to another relationship, so that's why the energy profile increased. Figure 7 illustrates the impact of the Ec on the temperature profile. The effect can be clearly seen in the graph. According to what is stated in it, an increase in the Ec values might result in an increased tendency in the energy profile. When viewed from a physical perspective, Ec is accountable for the production of pressures that come about by friction and ultimately result in an increase in the kinetic energy of the liquid. The impact of Pr is presented in Figure 8. According to our understanding, Pr has a negative impact on the value of the energy profile. The line graph on the diagram of the temperature profile shows a decreasing trend as the Pr value increases. According to our understanding, it is an occurrence of the speed of heat exchange between a liquid that is moving and a solid structure.

Fig. 9 demonstrate that the effects of the M and K on the *CF*. The figure indicates that decreased when increases the porosity values, because it acts as to decrease the fluid movement by the frictional forces. While the opposite trend we noticed when increasing the Rd vales which is presented in Fig. 10. The streamlines are plotted for different values of M (0.5, 1.0), which is demonstrated in Fig. 11.

Table 2. Validation table for different Pr of the present investigation.

Pr	Ali et al. [13]	Present results
0.7	0.4560	0.455561
2.0	0.9113	0.910026
7.0	1.8954	1.895692

5. Conclusion

The present investigation work explored the numerical solution for MHD of Al_2O_3-Cu mixed nanofluid over a stretching surface. The bvp5c technique was used to solve the issue of velocity, temperature and the outcome was really the solution to the problem. And also, in order to validate the active impact of important parameters, outlines are plotted. The results are presented in nemours kinds of profile types, including a 2D plot, contours and streamlines.

The following list includes the study's noteworthy results:

- Velocity outline declined for the higher values of the *M* parameter, on the other hand we noticed the opposite tendency in energy outline.
- Enhancement in radiation parameter will enhance the temperature profile.
- The skin friction factor decreases for the larger values of the porosity parameter.
- The Nusselt number profile increased, for the higher values of the *Rd* parameter.
- Streamlines have an oscillating character, which is necessary for magnifying the various values of *M*.

References

[1] Y. X. Li *et al.*, "Dynamics of aluminum oxide and copper hybrid nanofluid in nonlinear mixed Marangoni convective flow with entropy generation: Applications to renewable energy," *Chinese J. Phys.*, vol. 73, no. June, pp. 275–287, 2021, doi: 10.1016/j.cjph.2021.06.004.

[2] G. Ramasekhar and P. B. A. Reddy, "Numerical analysis of significance of multiple shape factors in Casson hybrid nanofluid flow over a rotating disk," *Int. J. Mod. Phys. B*, Oct. 2022, doi: 10.1142/S0217979223501138.

[3] G. Ramasekhar and P. Bala Anki Reddy, "Entropy generation on Darcy–Forchheimer flow of Copper-Aluminium oxide/Water hybrid nanofluid over a rotating disk: Semi-analytical and numerical approaches," *Sci. Iran.*, vol. 30, no. 6, pp. 2245–2259, 2023, doi: 10.24200/sci.2023.60134.6617.

[4] S. Jakeer and S. R. R. Reddy, "Electrokinetic membrane pumping flow of hybrid nanofluid in a vertical microtube with heat source/sink effect," *Eur. Phys. J. Plus*, vol. 138, no. 6, p. 489, Jun. 2023, doi: 10.1140/EPJP/S13360-023-04118-7.

[5] R. Reddy, R. G.-E. E. J. of Physics, and undefined 2023, "Enhanced Heat Transfer Analysis on MHD Hybrid Nanofluid Flow Over a Porous Stretching Surface: An Application to Aerospace Features," *Period. Reddy, R GunisettyEast Eur. J. Physics, 2023•periodicals.karazin.ua*, vol. 4, pp. 286–293, 2023, doi: 10.26565/2312-4334-2023-4-36.

[6] S. R. Reddisekhar Reddy, S. Jakeer, V. E. Sathishkumar, H. T. Basha, and J. Cho, "Numerical study of TC4-NiCr/EG+Water hybrid nanofluid over a porous cylinder with Thompson and Troian slip boundary condition: Artificial neural network model," *Case Stud. Therm. Eng.*, vol. 53, p. 103794, Jan. 2024, doi: 10.1016/J.CSITE.2023.103794.

[7] U. S. Mahabaleshwar, E. H. Aly, and T. Anusha, "MHD slip flow of a Casson hybrid nanofluid over a stretching/shrinking sheet with thermal radiation," *Chinese J. Phys.*, vol. 80, no. March, pp. 74–106, 2022, doi: 10.1016/j.cjph.2022.06.008.

[8] S. Jakeer and P. Bala Anki Reddy, "Entropy generation on EMHD stagnation point flow of hybrid nanofluid over a stretching sheet: Homotopy perturbation solution," *Phys. Scr.*, vol. 95, no. 12, p. p.125203, Oct. 2020, doi: 10.1088/1402-4896/abc03c.

[9] S. Jakeer, P. BalaAnki Reddy, A. M. Rashad, and H. A. Nabwey, "Impact of heated obstacle position on magneto-hybrid nanofluid flow in a lid-driven porous cavity with Cattaneo-Christov heat flux pattern," *Alexandria Eng. J.*, vol. 60, no. 1, pp. 821–835, Feb. 2021, doi: 10.1016/j.aej.2020.10.011.

[10] R. Rehman, H. A. Wahab, and U. Khan, "Heat transfer analysis and entropy generation in the nanofluids composed by Aluminum and γ− Aluminum oxides nanoparticles," *Case Stud. Therm. Eng.*, vol. 31, p. 101812, Mar. 2022, doi: 10.1016/j.csite.2022.101812.

[11] Hayat and et al., "Thermo-diffusion and diffusion thermo analysis for Darcy Forchheimer flow with entropy generation," *Ain Shams Eng. J.*, vol. 13, no. 1, p. 101530, Jan. 2022, doi: 10.1016/J.ASEJ.2021.06.016.

[12] G. Ramasekhar and P. B. A. Reddy, "Semi-analytical and numerical explorations on entropy optimization of EMHD in Casson hybrid nanofluid with radiation slip and convective boundary conditions," *Waves in Random and Complex Media*, 2022, doi: 10.1080/17455030.2022.2144656.

[13] M. Ramzan, F. Ali, N. Akkurt, A. Saeed, P. Kumam, and A. M. Galal, "Computational assesment of Carreau ternary hybrid nanofluid influenced by MHD flow for entropy generation," *J. Magn. Magn. Mater.*, vol. 567, no. October 2022, p. 170353, 2023, doi: 10.1016/j.jmmm.2023.170353.

[14] G. Ramasekhar and P. B. A. Reddy, "Entropy generation on EMHD Darcy-Forchheimer flow of Carreau hybrid nano fluid over a permeable rotating disk with radiation and heat generation : Homotopy perturbation solution," *Proc. Inst. Mech. Eng. Part E J. Process Mech. Eng.*, 2022, doi: 10.1177/09544089221116575.

[15] K. G. Kumar, N. G. Rudraswamy, B. J. Gireesha, and S. Manjunatha, "Non linear thermal radiation effect on Williamson fluid with particle-liquid suspension past a stretching surface," *Results Phys.*, vol. 7, pp. 3196–3202, 2017, doi: 10.1016/j.rinp.2017.08.027.

[16] A. M. Rashad, A. J. Chamkha, M. A. Ismael, and T. Salah, "Magnetohydrodynamics Natural Convection in a Triangular Cavity Filled with a Cu-Al2O3/Water Hybrid Nanofluid with Localized Heating from below and Internal Heat Generation," *J. Heat Transfer*, vol. 140, no. 7, Jul. 2018, doi: 10.1115/1.4039213/384910.